

UV–visible absorption of small gold clusters in neon: Au_n (n = 1–5 and 7–9)S. Lecoultre,¹ A. Rydlo,¹ C. Félix,³ J. Buttet,¹ S. Gilb,² and W. Harbich^{1,a)}¹*Institut de Physique de la Matière Condensée, École Polytechnique Fédérale de Lausanne, 1015 Lausanne, Switzerland*²*MS-ROK Research Informatics, Merck KGaA Frankfurter Str. 250 64293 Darmstadt, Germany*³*Meteo Swiss, 1530 Payerne, Switzerland*

(Received 12 October 2010; accepted 8 December 2010; published online 15 February 2011)

We present optical absorption spectra in the UV–visible range ($1.5 \text{ eV} < E < 6 \text{ eV}$) for mass selected neutral gold clusters Au_n ($n = 1-5$ and $7-9$) embedded in solid Ne at 7 K. The experimental spectra are compared with time-dependent density functional calculations. Electronic transitions are distributed over the whole energy range without any concentration of the oscillator strength in a small energy window, characteristic for the more *s*-like metals such as the alkalis or silver. Contrary to the case of silver and partly copper clusters, transitions issued from mainly *d*-type states are significantly involved in low energy transitions. The measured integrated cross section is smaller (<20%) than expected from a free-electron system, manifesting the strong screening of the *s* electrons due to the proximity of the *s* and *d* levels in gold. © 2011 American Institute of Physics. [doi:10.1063/1.3537739]

I. INTRODUCTION

The size-dependent evolution of the structural, physical, and chemical properties of finite size aggregates has been the subject of continuing basic and applied research interests. Since the beginning, optical spectroscopy has been a powerful technique to study the electronic and, via the comparison to calculations, the structural properties of metal clusters.

From a fundamental point of view, clusters of noble metal elements are of particular interest because they form the natural bridge between “simple” and transition-metal clusters, and thus constitute an interesting ground for the testing of theoretical approaches. Furthermore, the study of a heavy metal such as gold requires the inclusion of relativistic effects. So far the experimental study of the optical absorption of neutral noble metal clusters beyond the trimer was limited to Ag clusters, which have a cross section more than five times higher than that of gold and copper clusters. Improvements in the experimental sensitivity¹ and the use of very weakly interacting neon matrices² make the other noble metal clusters accessible to the experiment.

Recently, a surge of activity was devoted to the study of Au_n clusters, both neutral and ionized. This is related to the finding that gold nanoparticles and in particular very small gold clusters containing as few as 7–8 atoms show pronounced catalytic activity^{3–6} and remarkable luminescent properties.^{7–11} A number of theoretical calculations^{12–16} predict, contrary to alkali metal clusters, the persistence of planar structures as the energetically favorable conformation up to a large number of atoms, depending on the charge state of the Au_n clusters. This behavior, which is not found in the case of the other noble metal clusters,^{13,17} has been correlated with relativistically enhanced *s*-*d* hybridization and *d*-*d* interaction.^{18,19}

In the case of charged clusters these theoretical predictions were compared to ion mobility measurements,^{20,21} photoelectron spectroscopy studies,¹⁵ photodissociation spectroscopy of Au_n[−]Xe, (Ref. 22) and Au_m⁺Ar clusters²³ as well as by trapped ion electron diffraction.²⁴ There are fewer techniques which give access to the structure of neutral clusters. Recently, Gruene *et al.*²⁵ studied Au₇, Au₁₉, and Au₂₀ aggregates in the gas phase by vibrational spectroscopy, their measurements for Au₇ are compatible with a planar edge-capped triangle with C_s symmetry. High quality absorption spectra of neutral clusters when compared to reliable theoretical calculations also give access to the structure of the lowest energy isomer as was shown in the case of Na (Refs. 26 and 27) and Ag (Refs. 28–30) clusters. This is, however, a more difficult task for Cu (Ref. 32) and Au clusters.

We present in this paper the absorption spectra that were obtained for Au_n ($n = 1-5$ and $7-9$) clusters condensed in a Ne matrix at 7 K. These spectra present the first systematic study of the absorption spectra containing more than three atoms in a weakly interacting environment. Recent (TD-DFT) time dependent density functional theory calculations of the absorption spectra of Au_n ($n = 2-14$) (Ref. 31), as well as own calculations with the b3-lyp functional, which is also suitable for the description of Ag clusters³² are compared to the experimental data.

We find that the gold absorption spectra present a large amount of transitions spread over a wide energy range. Agreement with TD-DFT calculations is poor and does not allow to attribute the optical spectra to a specific isomer as it is the case in the more *s*-like Ag clusters.

II. EXPERIMENTAL AND COMPUTATION

Clusters are formed from a metal target sputtered by a 10 mA Xe⁺ ion beam at 25 keV. The gold cations are extracted by an electrostatic lens system and focused into a

a)Electronic mail: wolfgang.harbich@epfl.ch.

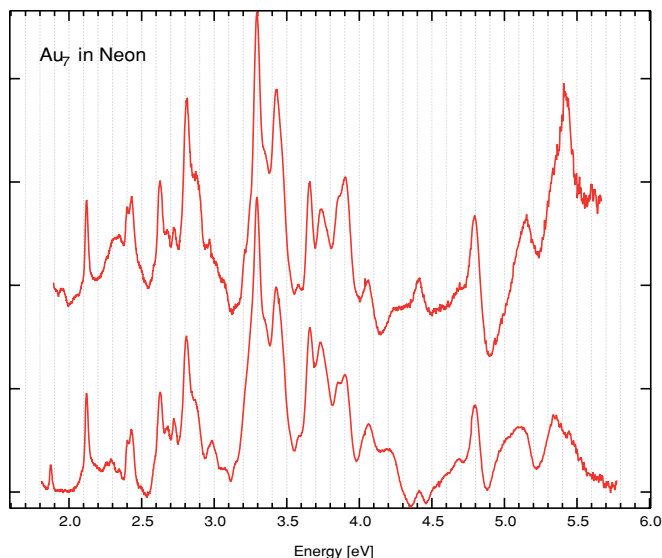


FIG. 1. Absorption spectra for two different depositions of Au₇.

“Bessel box” type (BB) energy filter which also acts as a beam stop for the intense flux of neutral clusters. The cations of interest are mass-selected and directed toward the sample holder, which consists of a superpolished aluminium mirror (Valley design corp.). The sample holder is fixed to a cold head cryostat (SRP-052A Cryocooler, Sumitomo Heavy Industries Ltd.) that allows refrigeration to about 7 K. Size-selected clusters are codeposited with Ne at a dilution of $1:3 \times 10^5$. The matrix has a thickness of 50 μm .

Optical absorption measurements are performed by injecting light through the 2 mm length of the matrix and collecting the transmitted light on the other side with an optical fiber of 400 μm core diameter. The collected light is analyzed by an optical spectrometer coupled with a liquid-nitrogen-cooled charge coupled device (CCD). Comparing the intensity of the light passing through a matrix doped with clusters with a reference signal of light passing through a pure neon matrix yields the absorption spectrum. Typical numbers of deposited charges inside the matrix are comprised between 8 nAh for the dimer and 450 pAh for the octamer, corresponding respectively to cluster densities of $3.6 \times 10^{15}/\text{mm}^3$ (dilution of $1:3 \times 10^5$) and $2 \times 10^{14}/\text{mm}^3$ (dilution of $1:5 \times 10^6$).

Since the absorption spectra show intense and well-defined peaks together with a large number of fine structures, it is important to determine whether the observed fine structures are part of the absorption spectra or correspond to artifacts. We present in Fig. 1 two absorption spectra of gold heptamers obtained from two different samples. The position of all structures, including the finer details, are reproduced on both spectra, while the relative intensity between the peaks may vary depending on the background signal. This is in particular true above 5 eV where the structures become broader and less resolved due to the lower intensity of the light transmitted through the matrix. The same conclusions can be drawn for all gold clusters spectra reported in Fig. 2.

In the present study TD-DFT was used to describe the electronic structure and the UV–vis absorption spectra of

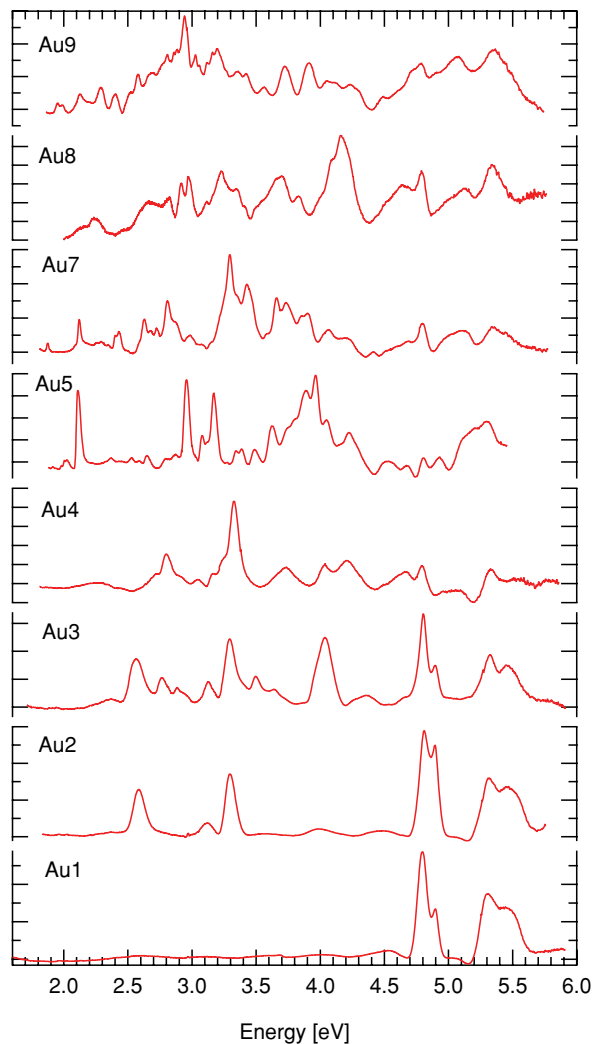


FIG. 2. Experimental absorption spectra of Au_{*n*}, *n* = 1–5, 7 and 9 obtained in a neon matrix at 7 K at an energy of typically 20 eV.

the Au clusters. A calculation scheme was used, which is equally suitable for other coinage metals. The b3-lyp (Refs. 33 and 34) functional together with the def2-TZVP basis ((8s7p6d1f)/[6s4p3d1f]) as implemented in the TURBOMOLE package was chosen.³⁵ To compare the calculations with the literature and to check consistency, a few sizes were repeated with the Perdew–Becke–Ernzerhof (PBE) functional. The inner 28 electrons were described using the respective ECP (effective core potential). Quadrature grids were of m3 quality.³⁶ The geometry optimization was started using structures found in the literature and at least the two lowest lying isomers from calculations by Fernandez¹³ were evaluated. The geometry optimizations are carried out with symmetry restriction where applicable. The TD-DFT calculations were performed with the ESCF module³⁷ of the TURBOMOLE V-5.9 program package.³⁸

III. RESULTS

Figure 2 presents the experimental spectra of small neutral gold clusters (Au_{*n*}, *n* = 1–5 and 7–9) deposited in a neon matrix at 7 K. The atom and the dimer spectra have already

been published together with their fluorescence spectra.³⁹ The hexamer has not been measured in this study because of its low abundance in the molecular beam.

Figure 3 summarizes the experimental results and the TD-DFT spectra of the lowest energy Au isomers obtained in the calculation scheme described above. The lower trace of Fig. 3 presents the “cleaned”, i.e., free of fragments, experimental spectra of Au_{*n*} (*n*=1–5, and 8). The raw spectra of Au_{*n*} contain spectroscopic traces of Au₁ and Au_{*n*-1}, due to fragmentation upon deposition. These contributions have been eliminated by deconvoluting the measured spectra in a sum of Gaussians. The absorption lines attributed to fragmentation have then been subtracted in order to obtain the “cleaned” absorption spectra for a given cluster size. This deconvolution was not possible however in the cases of Au₇ and Au₉ due to the very large number of observed narrow transitions with linewidths smaller than 20 meV. They are shown without signal treatment in these two cases.

Table I gives the peak position and the integrated cross section (in parenthesis) of the different transitions associated with the respective cluster size. The integrated cross section for a given transition was determined by integrating the corresponding absorption profile normalized by the cluster density. We estimate the absolute error to be of the order of 50%, while the relative error from one transition to the other for one cluster size is smaller.

TABLE I. Peak position (in eV) and integral of the cross section over the energy (in parenthesis) of the corresponding transition. The oscillator strength is obtained by multiplying the integrated cross section (10^{-18} cm² eV) by 1.12×10^{-2} .

Species	Peak position (oscillator strength) [eV] [(cm ² × 10 ⁻¹⁸)
Au ₁	4.80(3.90), 4.90(1.00), 5.30(2.16), 5.44(4.82),
Au ₂	2.58(2.24), 3.13(0.56), 3.30(2.35), 3.96(0.75),
Au ₃	2.36(0.82), 2.76(2.12), 2.88(0.60), 2.95(0.64), 3.50(2.17), 3.64(1.40), 4.04(6.02), 4.36(1.23), 4.70(1.28)
Au ₄	2.80(1.49), 3.05(0.56), 3.17(1.73), 3.25(0.84), 3.33(8.17), 3.73(5.20), 4.20(5.98), 4.49(0.37), 4.66(3.37)
Au ₅	2.02(0.23), 2.11(2.05), 2.37(0.09), 2.53(0.08), 2.59(0.02), 2.65(0.21), 2.87(0.50), 2.96(3.62), 3.08(1.68), 3.17(3.45), 3.27(0.28), 3.39(0.60), 3.49(1.09), 3.62(2.20), 3.74(3.40), 3.81(1.74), 3.89(4.79), 3.96(3.17), 4.05(3.54), 4.22(4.14), 4.53(0.46), 4.93(0.57), 5.11(1.92), 5.20(1.00),
Au ₇	1.87, 2.12, 2.40, 2.43, 2.63, 2.68, 2.72, 2.81, 2.88, 2.99, 3.29, 3.43, 3.58, 3.66, 3.73, 3.90, 4.06, 4.21, 4.41, 4.69, 5.10
Au ₈	2.15(0.18), 2.23(1.02), 2.66(2.94), 2.91(0.86), 2.97(2.12), 3.11(1.42), 3.23(3.49), 3.34(2.09), 3.42(0.10), 3.54(1.53), 3.69(4.26), 3.83(0.74), 4.01(1.00), 4.07(0.75), 4.17(8.17), 4.64(3.36), 5.12(1.73)
Au ₉	1.95, 1.99, 2.13, 2.29, 2.40, 2.58, 2.69, 2.81, 2.88, 2.94, 3.03, 3.06, 3.12, 3.16, 3.20, 3.36, 3.42, 3.57, 3.72, 3.91, 4.05, 4.12, 4.23, 4.49, 5.08

The TD-DFT spectra of the lowest lying Au isomers obtained in the calculation scheme described above are given in Fig. 3 (upper black traces). We have made a Mulliken population analysis of the states involved in the transitions in order to determine the principal *s*, *p*, or *d* contributions of the Kohn–Sham molecular orbitals involved in a given transition. Noted by a black dot are the absorption lines whose initial state is predominantly of *s* type, and we shall speak of *s*-*s* or *s*-*p* transitions depending on the principal *s* or *p* character of the final state. The remaining absorption lines, issued predominantly of the *d*-band, correspond to *d*-*s* or *d*-*p* transitions.

A. Absorption spectra and fragmentation

The deconvolution of the absorption spectra as described above yields the contents of fragments in the matrix by their optical fingerprint. We find, as expected,⁴⁰ decreasing fragmentation rates going from the dimer to the nonamer.

For the dimer (see Fig. 2) a strong signature of the atom is visible between 4.7 and 5.7 eV, it corresponds to a fragmentation rate of Au₂ into Au₁ estimated to about 50%. The corresponding Au₁ absorption lines (see Table I) are thus taken out of the Au₂ deconvoluted spectrum to obtain the “cleaned” Au₂ experimental spectrum. The experimental Au₃ spectrum in Fig. 2 also clearly shows the atom, as well as the dimer signature at 2.58, 3.13, and 3.30 eV. Note that even in reducing the deposition energy, it was not possible to obtain a lower fragmentation rate. This is related to the large energy spread of the clusters prepared by sputtering. The shapes of the Au₂ absorption spectrum between 4.7 and 5.7 eV are different from the absorption profile of the atom alone. This suggests that an additional Au₂ absorption signal around 4.9 eV is hidden by the presence of the atom. We shall show by comparison with known results that this is indeed the case. We have thus marked in Fig. 3 the energy range above 4.7 eV by an interrupted line. The same situation occurs for Au₃ in the same energy range, suggesting that here too a Au₃ transition is hidden by the presence of the atom.

For the tetramer, the low abundance of clusters in the beam is responsible for the inferior quality of the signal. Since the spectrum does not show any dimer signature, we can safely affirm that the dominant fragmentation channel is Au₄ → Au₃ + Au₁. This observation is confirmed by a second measurement of the same system deposited at higher kinetic energy. Fragmentation of the pentamer is not clearly visible on the absorption spectrum, even if one cannot exclude that the small peaks at 3.34, 4.81, and 5.3 eV are due to the tetramer and the atom, respectively. The experimental spectrum of Au₅ shows an especially high number of absorption peaks with peak widths that do not exceed 60 meV. Careful analysis shows that they can all be attributed to the pentamer.

All absorption spectra up to *n* = 9 show peaks at 4.80 and 5.33 eV, which reveal the presence of gold atoms in the neon matrix. Curiously, however, the signature of Au_{*n*-1} fragments is only discernible for *n* = 3–5 and inexistent for *n* = 7–9. We suggest that not only fragmentation is responsible for the signature of the Au atom on the optical spectra but also dissociation of the sputtered clusters. Indeed, we know that the hot clusters produced via a sputtering process cool down

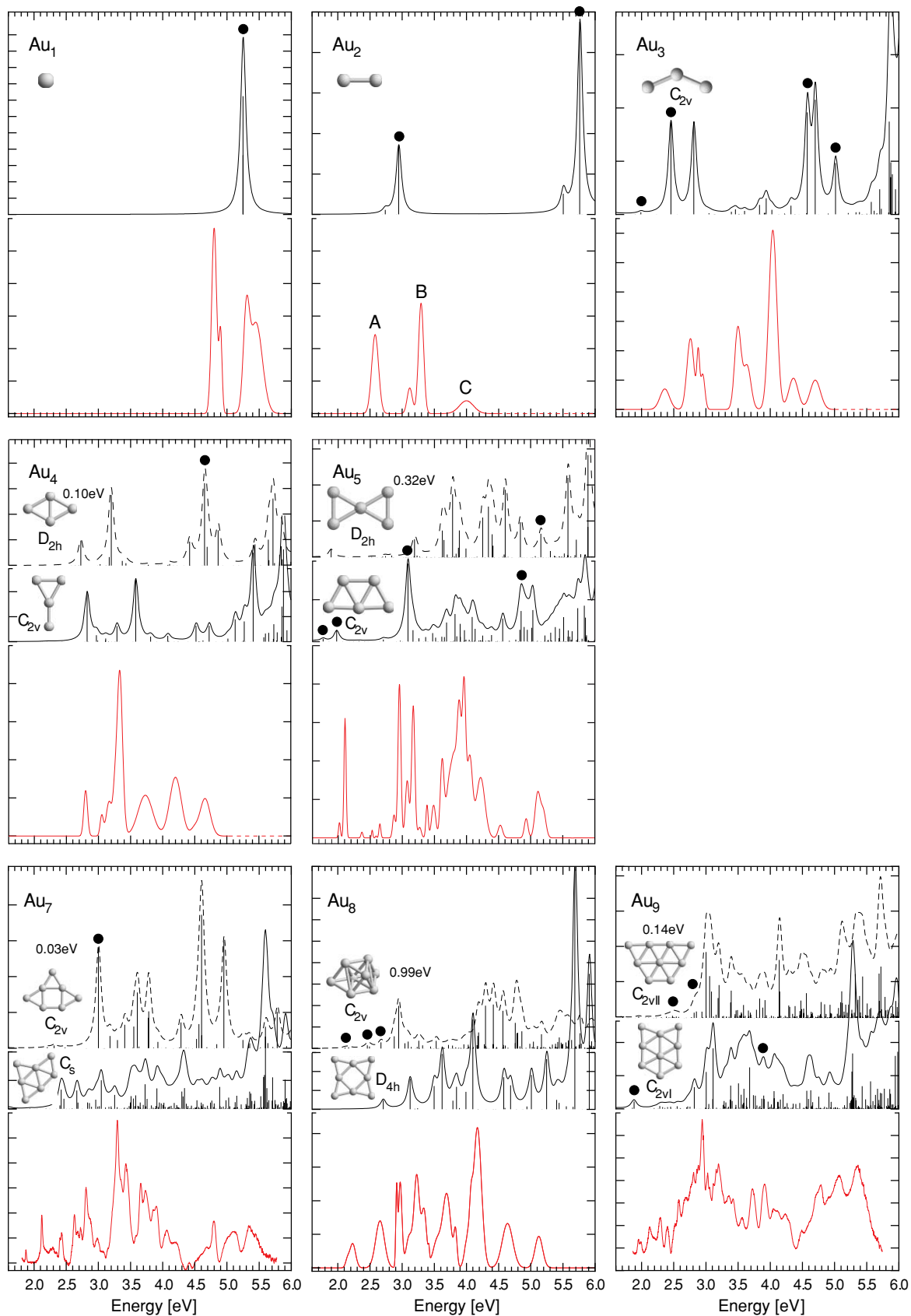


FIG. 3. Comparison between experimental and calculated absorption spectra of gold clusters. Experimental “cleaned” absorption (see text) for Au_n ($n = 1-5$ and 8) and without signal treatment ($n = 7$ and 9) lower curve. TD-DFT calculations for the ground state configuration-continuous black line- and next higher isomer-interrupted black line. The transitions have been enlarged by Lorentzians of 0.1 eV FWHM. The vertical scale for the calculated spectra is a measure of the oscillator strength per atom, one interval corresponding to 0.05 units for Au_1 and Au_2 , 0.025 units for Au_3 to Au_5 and 0.0125 units for Au_7 to Au_9 . The black dot identifies transitions whose initial state is predominantly of s-type.

by evaporation of atoms. If such evaporation takes place after the Bessel box, neutral atoms can contaminate the neon matrix since the ratio between the initial clusters velocity and the drift velocity after dissociation is small. By comparing our values to the experiments by Begemann⁴¹ on evaporative cooling of clusters produced by sputtering, we find that this phenomenon is very likely to happen in our case, leading to part of the observed atom signal.

B. Comparison with known experimental results

In what follows, we shall examine size by size the experimental absorption spectra, and compare them with known results when available, i.e., essentially up to the trimer. The absorption spectra for the other measured sizes are new.

Au₁. The experimental absorption spectra of the atom and dimer in neon have already been discussed in a previous publication.³⁹ We present here these spectra for completeness together with the corresponding TD-DFT calculations.

The experimental spectrum of gold atoms in neon shown in Fig. 3 contains two large structures of average position equal to 4.82 and 5.40 eV. Comparison with previous measurements in neon⁴² and in other matrices⁴³ confirms this spectrum except for the small secondary peak at 4.9 eV, which may be due to a less favorable second site isomer in the neon matrix.³⁹ The two large structures correspond to the spin-orbit split $2P_{1/2} \leftarrow 2S_{1/2}$ and $2P_{3/2} \leftarrow 2S_{1/2}$ transitions measured⁴⁴ respectively in gas phase at 4.63 and 5.11 eV.

Au₂. The Au dimer has been studied in the gas phase,^{45–47} in Ar (Refs 43 and 48) and in Kr (Ref. 49) matrices. The gas phase measurements have found several absorption bands, whose origins are situated at 2.07, 2.25, 2.44, 2.98, and 3.19 eV. With good certainty we attribute the peak measured at 2.58 eV to the so-called A←X absorption measured at 2.44 eV in gas phase and the peak measured at 3.30 eV to the B←X transition measured at 3.19 eV in gas phase. The weak absorption at 3.96 eV has also been observed in argon^{43,48} and krypton⁴⁹ matrices around 4.0 eV. It is, however, not visible in the gas phase, which suggests⁵⁰ that it is due to a symmetry forbidden transition, denoted by C, which becomes allowed by interaction with the matrix. The secondary peak at 3.13 eV has not been observed in other matrices. Fluorescence data³⁹ indicate that it is not due to a second site isomer. Comparison to gas phase measurements⁴⁷ suggests that it is related to the transition whose origin is situated at 2.98 eV. The measurements in argon⁴⁸ and krypton⁴⁹ matrices also find peaks situated around 5.0 and 5.9 eV. The 5.0 eV signal corresponds to the energy range in which we observe a strong signal due to atomic gold resulting from fragmentation of the dimer. This suggests, together with the different shapes of the atom and dimer signals, that a dimer peak hidden by the presence of atomic gold also exists in a neon matrix around 5.0 eV.

Au₃. The different lines (see Table I) attributed to the gold trimer give more details but they are in agreement with the previous measurements in Ar (Refs. 48 and 51) and Kr (Ref. 49) if we include a small matrix shift which may vary from one transition to the other, as shown in the case of Na clusters.⁵² In particular, there is a one to one corre-

spondence between the peaks reported by excitation spectroscopy in argon,⁴⁸ krypton,⁴⁹ and our measurements if we consider the two peaks at 3.50 and 3.64 eV as an enlarged single absorption line as well as the three peaks at 2.76, 2.88, and 2.95 eV. Note also that a transition reported in argon at 5.37 eV and in krypton at 5.32 eV is not clearly visible in our measurements. We suggest, as in the case of Au₂, that such a transition also exists in neon, but that it is hidden by the strong atomic signal resulting from fragmentation of Au₃.

Au₄. The gold tetramer absorption spectrum reported in Fig. 3 after subtraction of the Au₁ and a weak Au₃ signal is formed of two narrow peaks at 2.80 and 3.33 eV, weaker peaks at 3.05 and 3.17 eV, and broader peaks at 3.73, 4.20, and 4.66 eV. To our knowledge, no previous measurement of the neutral tetramer has been reported. Only photodissociation spectra of cationic Au van der Waals complexes [Au₄⁺Ar_n (n=0–4)] in the energy range of 2.14–3.35 eV are published.⁵³

Au₅. The absorption spectrum of the pentamer is composed of a large number of narrow peaks (see Table I). Zheng *et al.* have recently measured the absorption and emission lines from fluorescent water soluble Au₅ nanoclusters. The measured excitation energy equal to 3.76 eV is in reasonable agreement with the large absorption centered at 3.9 eV.

Au₇. The experimental absorption signal of the gold heptamer is composed of a large number of sharp transitions. The spectral width of the transitions are remarkably small, a number of transitions not larger than 30 meV can be observed, in particular at low energies. Note also that the high concentration of oscillator strength between 3 and 4 eV with intense structures probably composed of several transitions. The absorption spectrum of Au₇ has already been measured by Collings *et al.*⁵⁴ in a comparable energy range by photodepletion techniques of van der Waals complexes (Xe). The authors report mainly one large structureless absorption feature centered around 3.0 eV with a width of 0.8 eV. Most likely this reflects just the envelope of the numerous transitions we have observed in this energy range taking account the matrix shift.⁵⁵ Their data show a rising absorption above 4 eV attributed to the involvement of the *d*-electrons, which is not verified in our results.

The gas phase structure of Au₇ has very recently been unambiguously determined by Gruene *et al.*²⁵ using vibrational spectroscopy. The observed vibrational spectrum is in agreement with a planar C_s ground state configuration.

Au₈. The absorption of the gold octamer, when compared with that of the odd numbered clusters Au₅, Au₇, and Au₉, is composed of a small number of large peaks, comprised between 2.2 and 5.2 eV. A maximum of the absorption centered at 3.2 eV is in agreement with the excitation energy measured by Zheng *et al.* at the same energy, note however that in the present work the main absorption is rather situated at 4.1 eV.

Au₉. Finally, the experimental spectrum for the nonamer shows a large amount of peaks constituting the fine structure of broader absorption bands with local maxima at 2.94, 3.20, 3.72, 3.91, and 5.08 eV. The photodissociation spectra obtained by Collings *et al.*⁵⁴ show two broad absorption bands around 2.2 and 3.0 eV, which roughly correspond to maxima in the oscillator strength of our spectrum.

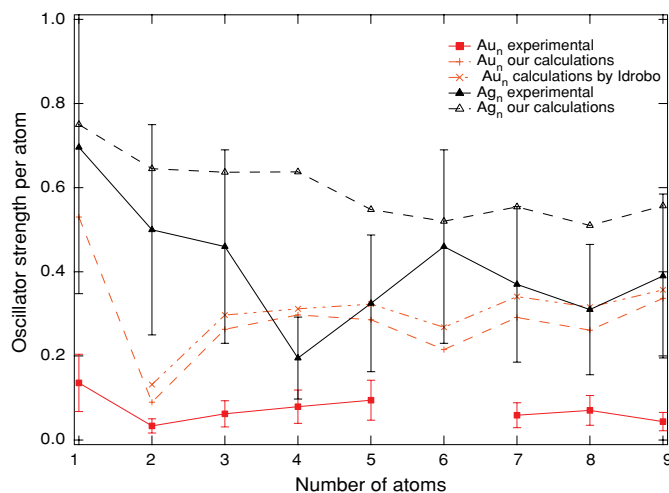


FIG. 4. Experimental and theoretical values of the oscillator strength per atom for Au_n clusters. The theoretical value has been reported for the ground state configuration, it is integrated up to 5.5 eV in our calculation and up to 6.0 eV in Idrobo's calculation.³¹ The systematic error of 50% on the measured absolute value is related to the uncertainty in determining the density of clusters per unit area and the non-negligible fragmentation. The experimental and calculated values of the oscillator strength for Ag_n clusters is taken from Ref. 32.

C. Comparison to TD-DFT calculations

Numerous calculations have been performed on small Au clusters. The gold dimer has been calculated, including the excited states, using Hartree–Fock and DFT methods.^{56–59} Similar techniques were applied to determine the ground state geometries of the trimer,^{60–63} the tetramer,^{60,62,64} and the pentamer.^{62,64} DFT calculations have been performed more recently in order to predict the lowest energy structures^{12–14,16,18,19,31} and to calculate the optical spectra by TFD-DFT for clusters up to Au_{14} and Au_{20} .³¹

Our calculations for the structures are given in Fig. 3 for the two lowest energy isomers, together with their energy difference. They are in close agreement with the ones reported in the literature, except for Au_4 in which we find that the “Y”-shaped structure has the lowest energy. However, the rhombus is only 0.1 eV higher in energy. Note that in agreement with previous calculations all ground state configurations are planar.

The TD-DFT absorption spectra of the two lowest lying isomers are also given in Fig. 3 (upper black traces). They are in qualitative agreement with the previous TD-DFT absorption spectra of Au_n ($n = 2–14$), although they differ in details. For example, Idrobo *et al.*³¹ found for Au_3 , one intense peak situated at 2.63 eV, rather than two peaks at 2.23 and 2.82 eV as in our calculation. More global quantities, such as the oscillator strength (see Fig. 4) are in close agreement in both calculations.

It appears at first sight that the agreement between TD-DFT and experiment is poor and renders difficult to assign with certainty the measured spectra to a given isomer. This is already true for Au_1 for which TD-DFT calculations give one single peak attributed to the $S \leftarrow P$ transition, as it does not account for spin–orbit coupling and possible small matrix effects. However, its position at 5.25 eV is in good

agreement with the average value measured in gas phase at 4.95 eV and in a neon matrix at 5.16 eV. The TD-DFT absorption spectrum of Au_2 given in Fig. 3 is similar to Idrobo's result if we include a shift of approximately 0.3 eV. However, neither results are in good agreement with the gas phase or matrix absorption spectra, in particular the two intense A and B transitions are not reproduced. It is worth to notice that more elaborate calculations^{56–58} which take explicitly into account the spin–orbit coupling are in much better agreement with the dimer gas phase experimental absorption spectra. This is a clear indication that the lack of spin–orbit splitting in the TD-DFT calculations results in a serious limitation to reproduce the experimental spectra.

One important feature of the measured absorption spectra, when compared to silver,^{30,32} is that the absorption spectra in gold are formed of a large number of peaks scattered over a large energy range. This is especially true for the clusters with an odd number of atoms ($n = 5, 7$, and 9). As an example 14 transitions have been measured between 2 and 6 eV in the case of silver pentamers in neon,³² whereas 24 transitions have been observed for the gold clusters in the same energy range. This is even more visible in the case of Au_7 and Au_9 , whose decomposition of spectral lines into Gaussians was not possible due to the exceedingly large number of narrow transitions. This suggests that for Au_5 and Au_7 the ground state structures, whose oscillator strength is shared among a large number of transitions, correspond well to the large number of observed peaks. In the case of Au_8 the number of transitions for the more symmetrical D_{4h} geometrical structure is smaller than that for the C_{2v} geometry, which is in good agreement with the relatively small number of observed peaks. Furthermore, the experimental and theoretical D_{4h} absorption spectra show analogies in the repartition of oscillator strength. In the case of Au_9 it is probable that several isomers are present in the matrix, since several structures close in energy were predicted.

IV. DISCUSSION

Gold is one of the three coinage metals with an atomic ground state configuration of $[Xe]4f^{14}5d^{10}6s^1$. In this sense, its electronic structure is similar to silver $[Kr]4d^{10}5s^1$ and copper $[Ar]3d^{10}4s^1$. A remarkable difference is, however, the energetic position of the nd levels which are approximately 2 eV below the $(n + 1)s$ levels in copper and gold but 4 eV in silver. The same situation is found in the limit of very large particles or bulk electronic structure. The s levels are extended to a large flat band and the atomic d -states develop in a much more localized d -band. The frontier orbital of the d -band is approximately 2 eV below the Fermi energy for gold and copper, but 4 eV for silver. The consequences are imminent in the optical spectra of large particles. Silver develops a strong well-defined plasmon absorption centered around 4 eV, followed by interband transitions to higher energies. This concentration of oscillator strength in the energy range of the surface plasmon in Ag is visible down to small cluster sizes ($n > 3$). The Au plasmon, however, is heavily perturbed by s - d hybridization effects,⁶⁵ which reflects in the absorption spectra of small Au clusters, whose oscillator strength is scattered over a large energy range, as mentioned before.

Idrobo *et al.*³¹ have made a detailed study of the roles played by the *d*-electrons in the optical spectra by comparing silver and gold clusters, i.e., (i) quenching of the oscillator strength by screening of the *s*-electrons and (ii) getting partially involved in low-energy excitations. They conclude on the basis of their calculations that the screening effect is significantly enhanced in Au_{*n*} clusters compared to Ag_{*n*} clusters. They also show that the involvement of the *d*-electrons in low energy excitations of Au_{*n*} will also increase. Both effects are related to the energetic position of the *d*-levels compared to the *s* levels, as mentioned above. We reach the same conclusions through our calculations, although they differ in details, e.g., the lowest transition in Au₂ is also predominantly of *d*-character, but is issued from the HOMO-2 orbital rather than the HOMO-1 orbital as in Idrobo's calculation. We have noticed by a dot in Fig. 3 the transitions which are issued from an orbital of predominant *s* character. Note however that, except for Au₂, all transitions marked by a dot also contain a sizeable part of *d*-character, including the lowest energy transitions.

In the case of the Ag_{*n*} clusters absorption spectra,^{30,32} we find that the experimental spectra are characterized by a small number of intense absorption lines situated below 4.5 eV and a more complex structure above 5 eV. The intense absorptions are in close agreement with the calculated *s*-type transitions, while the higher energy *d*-type transitions are not well reproduced by the calculation. In the case of Cu clusters (*n* > 4), the analysis suggests that the general behavior is similar to that of silver; however, the emergence of *d*-type transitions occurs around 3 eV and makes it more difficult to assign the measured absorption spectra to given isomers.³² In the case of Au the direct influence of *s-d* hybridization is important down to the lowest energy transitions, although, like in Cu clusters, the percentage of *d* character in the transitions increases above 3 eV.

Figure 4 presents the experimental and theoretical values of the sum of the oscillator strengths (OS) per atom for the Au_{*n*} clusters up to a cut-off energy of 5.5 eV. On the same graph, we report the measured integrated OS up to the same energy for Ag_{*n*} clusters. The OS for Au clusters is considerably smaller (factor 5 to 10) than for Ag_{*n*}. The reason is, as mentioned before, the screening of the *s*-electrons by the *d*-electrons in Au_{*n*} compared to Ag_{*n*}. This screening has been shown^{17,66} to quench the OS in noble metal clusters.

The influence of the matrix and more particularly its effect on the OS (Ref. 52), however, cannot be neglected. We note that the OS of the *s* → *p* transition in neon, equal to 0.14 with an uncertainty of 50%, does not agree with the gas phase value of 0.52 (Ref. 44). A similar situation occurs in the case of Cu₁ in neon,³² while for atomic silver the measured OS of the *s-p* transition in the gas phase (0.72) (Ref. 44) is very close to the matrix value (0.71). Such a difference between the gas phase and the matrix values has already been reported by Gruen *et al.*⁶⁷ They found that the OS of Au atoms in Ar, Kr, and Xe matrices decreases by a factor of 1.2, 1.8, and 2.5, respectively. This implies that in the case of copper and gold, where the effect of the *s-d* hybridization is larger than in silver, the screening of the *s* electrons is modified by the presence of the matrix. This is also true for small Au_{*n*} and Cu_{*n*} clusters, in particular the two-dimensional geometrical struc-

ture of gold clusters certainly tends to enhance the effect of the interaction with the matrix. We also notice that, despite the uncertainty in the determination of the OS, the theoretical value is larger than the measured one by a factor comprised between 2 and 5. These differences are in part due to the effect of the matrix, they also indicate that the TD-DFT scheme does not reproduce well, the transitions in which a strong *d* component occurs.

V. CONCLUSION

We have presented optical absorption spectra of mass selected neutral Au_{*n*} (*n* = 1–9) clusters in the UV–visible range embedded in a solid neon matrix. We observe fingerprint spectra for each cluster size with very narrow (20 meV) optical transitions. The smaller energetic separation between the 6*s*¹ and 5*d*¹⁰ states in the atom, which evolves in a *d* band which is much closer to the Fermi energy than in silver, results in a strong influence of the *d*-electrons on the electronic transitions (screening of the *s* electrons and direct involvement in low energy transitions). This is well reproduced in the optical spectra. They show a much higher complexity and a larger number of transitions, in particular in the visible part of the spectrum, compared to similar sizes of silver clusters. A concentration of the oscillator strength in a small energy window, observed in alkali metals and silver, and interpreted in the collective excitation of valence electrons model, is absent in the case of Au clusters.

Our measurements have been compared to TD-DFT calculations available in the literature and to the present TD-DFT calculations. They reproduce several features, such as the large number of transitions and their distribution over the whole UV–visible spectrum. Comparison between experiment and theory does not, however, allow with certainty attribution of the measurements to specific isomers. More refined calculations taking explicitly into account spin–orbit and possibly matrix interaction effects are necessary. We suggest that the present measurements are of sufficient quality to be used as benchmark to test the validity of different theoretical approaches.

ACKNOWLEDGMENTS

This work has been supported by the Swiss National Science Foundation.

¹F. Conus, J. T. Lau, V. Rodrigues, and C. Félix, *Rev. Sci. Instrum.* **77**, 113103 (2006).

²S. Lecoulre, Ph.D. thesis (EPFL, Lausanne, CH, 2009).

³M. Valden, X. Lai, and W. Goodman, *Science* **281**, 1647 (1998).

⁴A. Sanchez, S. Abbet, U. Heiz, W.-D. Schneider, H. Häkkinen, R. N. Barnett, and U. Landman, *J. Phys. Chem.* **103**, 9573 (1999).

⁵C. T. Campbell, *Science* **306**, 234 (2004).

⁶B. Yoon, H. Häkkinen, U. Landman, A. S. Woz, J.-M. Antontietti, S. Abbet, K. Judai, and U. Heiz, *Science* **307**, 403 (2005).

⁷J. P. Wilcoxon, J. E. Martin, F. Parsapour, B. Wiedenman, and D. F. Kelley, *J. Chem. Phys.* **108**, 9137 (1998).

⁸T. P. Bigioni, R. L. Whetten, and O. Dag, *J. Phys. Chem. B* **104**, 6983 (2000).

⁹J. Zheng, J. T. Petty, and R. M. Dickson, *J. Am. Chem. Soc.* **125**, 7780 (2003).

- ¹⁰J. Zheng, C. Zhang, and R. M. Dickson, *Phys. Rev. Lett.* **93**, 077402 (2004).
- ¹¹P. R. N. J. Zheng and R. M. Dickson, *Annu. Rev. Phys. Chem.* **58**, 409 (2007).
- ¹²F. Remacle and E. S. Kryachko, *J. Chem. Phys.* **122**, 044304 (2005).
- ¹³E. M. Fernández, J. M. Soler, I. L. Garzón, and L. C. Balbás, *Phys. Rev. B* **70**, 165403 (2004).
- ¹⁴J. Zhao, J. Yang, and J. G. Hou, *Phys. Rev. B* **67**, 085404 (2003).
- ¹⁵H. Häkkinen, B. Yoon, U. Landman, X. Li, H.-J. Zhai, and L.-S. Wang, *J. Phys. Chem. A* **107**, 6168 (2003).
- ¹⁶H. Häkkinen and U. Landman, *Phys. Rev. B* **62**, 2287 (2000).
- ¹⁷S. Ogüt, J. C. Idrobo, J. Jellinek, and J. Wang, *J. Cluster Sci.* **17**, 609 (2006).
- ¹⁸H. Häkkinen, M. Moseler, and U. Landman, *Phys. Rev. Lett.* **89**, 033401 (2002).
- ¹⁹H. Grönbeck and W. Andreoni, *Chem. Phys.* **262**, 1 (2000).
- ²⁰F. Furche, R. Ahlrichs, P. Weis, C. Jacob, S. Gilb, T. Bierweiler, and M. M. Kappes, *J. Chem. Phys.* **117**, 6982 (2002).
- ²¹S. Gilb, P. Weis, F. Furche, R. Ahlrichs, and M. M. Kappes, *J. Chem. Phys.* **116**, 4094 (2002).
- ²²S. Gilb, K. Jacobsen, D. Schooss, F. Furche, R. Ahlrichs, and M. M. Kappes, *J. Chem. Phys.* **121**, 4619 (2004).
- ²³A. N. Gloess, H. Schneider, J. M. Weber, and M. M. Kappes, *J. Chem. Phys.* **128**, 114312 (2008).
- ²⁴X. Xing, B. Yoon, U. Landmann, and J. H. Parks, *Phys. Rev. B* **74**, 165423 (2006).
- ²⁵P. Gruene, D. M. Rayner, B. Redlich, A. F.G. van der Meer, J. T. Lyon, G. Meijer, and A. Fielicke, *Science* **321**, 674 (2008).
- ²⁶V. Bonačić-Koutecký, J. Pittner, C. Scheuch, M. F. Guest, and J. Koutecký, *J. Chem. Phys.* **96**, 7938 (1992).
- ²⁷J.-O. Joswig, L. Tunturivuori, and R. Nieminen, *J. Chem. Phys.* **128**, 014707 (2008).
- ²⁸V. Bonačić-Koutecký, V. Veyret, and R. Mitrić, *J. Chem. Phys.* **115**, 10450 (2001).
- ²⁹V. Bonačić-Koutecký, J. Pittner, M. Boiron, and P. Fantucci, *J. Chem. Phys.* **110**, 3876 (1999).
- ³⁰M. Harb, F. Rabilloud, D. Simon, A. Rydlo, S. Lecoultre, F. Conus, V. Rodrigues, and C. Félix, *J. Chem. Phys.* **129**, 194108 (2008).
- ³¹J. C. Idrobo, W. Walkosz, S. F. Yip, S. Ogut, J. Wang, and J. Jellinek, *Phys. Rev. B* **76**, 205422 (2007).
- ³²S. Lecoultre, J. Rydlo, A. Buttet, C. Félix, S. Gilb, and W. Harbich, *J. Chem. Phys.* **134**, 074303 (2011).
- ³³A. Becke, *Phys. Rev. A* **38**, 3098 (1988).
- ³⁴C. Lee, W. Yang, and R. Parr, *Phys. Rev. B* **37**, 785 (1988).
- ³⁵F. Weigend and R. Ahlrichs, *Phys. Chem. Chem. Phys.* **7**, 3297 (2005).
- ³⁶O. Treutler and R. Ahlrichs, *J. Chem. Phys.* **102**, 346 (1995).
- ³⁷R. Bauernschmitt and R. Ahlrichs, *Chem. Phys. Lett.* **256**, 454 (1996).
- ³⁸R. Ahlrichs, M. Bar, M. Haser, H. Horn, and C. Kolmel, *Chem. Phys. Lett.* **162**, 165 (1989).
- ³⁹S. Lecoultre, A. Rydlo, C. Félix, and W. Harbich, *Eur. Phys. J. D* **52**, 187 (2009).
- ⁴⁰S. Fedrigo, W. Harbich, and J. Buttet, *Phys. Rev. B* **58**, 7428 (1998).
- ⁴¹W. Begemann, K. H. Meiwes-Broer, and H. O. Lutz, *Phys. Rev. Lett.* **56**, 2248 (1986).
- ⁴²D. M. Gruen and J. K. Bates, *Inorg. Chem.* **16**, 2450 (1977).
- ⁴³W. E. Klotzbücher and G. A. Ozin, *Inorg. Chem.* **19**, 3767 (1980).
- ⁴⁴J. E. Sansonetti and W. C. Martin, *Handbook of Basic Atomic Spectroscopic Data* (National Institute of Standards and Technology, Gaithersburg, 2005).
- ⁴⁵J. Ruamps and R. Hebd, C.R.A.S. **238**, 1489 (1954).
- ⁴⁶L. L. Ames and R. F. Barrow, *Trans. Faraday Soc.* **63**, 39 (1967).
- ⁴⁷G. A. Bishe and M. D. Morse, *J. Chem. Phys.* **95**, 5646 (1991).
- ⁴⁸S. Fedrigo, W. Harbich, and J. Buttet, *J. Chem. Phys.* **99**, 5712 (1993).
- ⁴⁹W. Harbich, S. Fedrigo, and J. Buttet, *J. Chem. Phys.* **96**, 8104 (1992).
- ⁵⁰J. Wang, G. Wang, and J. Zhao, *Phys. Rev. B* **66**, 035418 (2002).
- ⁵¹G. A. Ozin, H. Huber, and S. A. Mitchell, *Inorg. Chem.* **18**, 2932 (1979).
- ⁵²B. Gervais, E. Giglio, E. Jacquet, A. Ipatov, P.-G. Reinhard, F. Fehrer, and E. Suraud, *Phys. Rev. A* **71**, 015201 (2005).
- ⁵³A. Schweizer, J. M. Weber, S. Gilb, H. Schneider, D. Schooss, and M. M. Kappes, *J. Chem. Phys.* **119**, 3699 (2003).
- ⁵⁴B. A. Collings, K. Athanassenas, D. Lacombe, D. M. Rayner, and P. A. Hackett, *J. Chem. Phys.* **101**, 3506 (1994).
- ⁵⁵S. Fedrigo, W. Harbich, and J. Buttet, *Int. J. Mod. Phys. B* **6**, 23 (1992).
- ⁵⁶W. C. Ermler, Y. S. Lee, and K. S. Pitzer, *J. Chem. Phys.* **70**, 293 (1978).
- ⁵⁷I. Itkin and A. Zaitsevskii, *Chem. Phys. Lett.* **374**, 143 (2003).
- ⁵⁸F. Wang, T. Ziegler, E. Lenthe, S. Gisbergen, and E. J. Baerends, *J. Chem. Phys.* **122**, 204103 (2005).
- ⁵⁹X. Wang, X. Wan, H. Zhou, S. Takami, M. Kubo, and A. Miyamoto, *J. Mol. Struct.* **579**, 221 (2002).
- ⁶⁰K. Balasubramanian, *J. Mol. Struct.* **292**, 291 (1989).
- ⁶¹H. Partridge, C. Bauschlicher, and S. Langhoff, *Chem. Phys. Lett.* **175**, 531 (1990).
- ⁶²V. Bonačić-Koutecký, J. Burda, R. Mitrić, M. Ge, G. Zampella, and P. Fantucci, *J. Chem. Phys.* **117**, 3120 (2002).
- ⁶³R. Wesendrup, T. Hunt, and P. Schwerdtfeger, *J. Chem. Phys.* **112**, 9356 (2000).
- ⁶⁴C. W. Bauschlicher, S. R. Langhoff, and H. Partridge, *J. Chem. Phys.* **93**, 8133 (1990).
- ⁶⁵U. Kreibitz and M. Vollmer, *Optical Properties of Metal Clusters*, Springer Series in Material Science Vol 25 (Springer, Berlin, 1995).
- ⁶⁶J. C. Idrobo, S. Ogut, K. Nemeth, J. Jellinek, and R. Ferrando, *Phys. Rev. B* **75**, 233411 (2007).
- ⁶⁷D. M. Gruen, S. L. Gaudioso, R. L. McBeth, and J. L. Lerner, *J. Chem. Phys.* **60**, 89 (1974).